Challenges in Panchromatic Modelling with Next Generation Facilities
Proceedings IAU Symposium No. 341, 2018
M. Boquien, E. Lusso, C. Gruppioni & P. Tissera, eds.

doi:10.1017/S1743921319002898

The diagnostic power of radio spectra from star-forming galaxies

Eric J. Murphy

National Radio Astronomy Observatory, 520 Edgemont Road,
Charlottesville, VA 22901, U.S.A.
email: emurphy@nrao.edu

Abstract. Radio continuum emission from galaxies is powered by a combination of distinct physical processes, each providing unique diagnostic information. Over frequencies spanning ∼1−120 GHz, radio spectra of star-forming galaxies are primarily comprised of: (1) non-thermal synchrotron emission powered by accelerated cosmic-ray electrons/positrons; (2) free-free emission from young massive star-forming (HII) regions; (3) anomalous microwave emission, which is a dominant, but completely unconstrained, foreground in cosmic microwave background experiments; and (4) cold, thermal dust emission that accounts for most of the dust and total mass content in the interstellar medium in galaxies. In this proceeding, we discuss these key energetic processes that contribute to the radio emission from star-forming galaxies, with an emphasis on frequencies $\gtrsim$ 30 GHz, where current investigations of star formation within nearby galaxies show that the free-free emission begins to dominate over non-thermal synchrotron emission. We also discuss how planned radio facilities that will access these frequencies, such as a next-generation Very Large Array (ngVLA), will be transformative to our understanding of the star formation process in galaxies.

Keywords. Star Formation, Radio Continuum

1. Introduction

Radio continuum observations have proven to be a workhorse in our understanding of the star formation process (i.e., stellar birth and death) from galaxies both in the nearby universe and out to the highest redshifts. Despite the fact that radio continuum emission is energetically weak with respect to a galaxy's bolometric luminosity, it provides critical information on the process of massive star formation, as well as a mechanism to access the relativistic [magnetic field + cosmic rays (CRs)] component in the interstellar medium (ISM) of galaxies. Stars more massive than ∼8 $M_{\odot}$ end their lives as core-collapse supernovae, whose remnants are thought to be the primary accelerators of CR electrons (e.g., Koyama *et al.* 1995) giving rise to the diffuse synchrotron emission observed from star-forming galaxies (Condon 1992). These same massive stars are also responsible for the creation of HII regions that produce radio free-free emission, whose strength is directly proportional to the production rate of ionizing (Lyman continuum) photons.

Radio frequencies spanning ∼1−120 GHz, which are observable from the ground, are particularly useful in probing such processes. The non-thermal emission component typically has a steep spectrum ($S_{\nu} \propto \nu^{\alpha}$, where $\alpha \sim -0.8$; e.g., Condon 1992), while the thermal (free-free) component is relatively flat ($\alpha \sim -0.1$). Accordingly, for globally integrated measurements of star-forming galaxies, lower frequencies (e.g., 1.4 GHz) are generally dominated by non-thermal emission, while the observed thermal fraction of the emission increases with frequency, eventually being dominated by free-free emission once beyond ∼30 GHz (Condon & Yin 1990). On ∼100 pc scales, the thermal fraction at

33 GHz for typical star-forming regions can be considerably higher, being $\gtrsim$80% (Murphy *et al.* 2011; Linden *et al.* 2020). Thus, observations at such frequencies, which are largely unbiased by dust, provide an excellent diagnostic for the current star formation rate (SFR) of galaxies.

It is worth noting that the presence of an anomalous microwave emission (AME) component in excess of free-free emission between ∼10 and 90 GHz, generally attributed to electric dipole rotational emission from ultrasmall ($a \lesssim 1$ nm) grains (Erickson 1957; Draine & Lazarian 1998; Planck Collaboration *et al.* 2011; Hensley & Draine 2017) or magnetic dipole emission from thermal fluctuations in the magnetization of interstellar dust grains (Draine & Lazarian 1999; Hensley *et al.* 2016), may complicate this picture. For a single outer-disk star-forming region in NGC 6946, Murphy *et al.* (2010) reported an excess of 33 GHz emission relative to what is expected given existing lower frequency radio data. This result has been interpreted as the first detection of so-called "anomalous" dust emission outside of the Milky Way. More recently, by surveying a sample of 112 star-forming complexes at 33 GHz in 56 nearby galaxies with the VLA at ∼2″ angular resolution as part of the Star Formation in Radio Survey (SFRS; Murphy *et al.* 2018a), resulting in the detection of 225 discrete sources, a second detection of AME was found in a compact, optically-faint region of NGC 4725 (Murphy *et al.* 2018b). Since this initial discovery in NGC 6946, a number of searches for extragalactic AME have been undertaken with WMAP and *Planck* data (e.g., the Magellanic Clouds, Bot *et al.* 2010; NGC 4945, Peel *et al.* 2011), all of which have been inconclusive, suggesting that this emission component is most likely sub-dominant for globally integrated measurements.

Due to the faintness of galaxies at high (i.e., $\gtrsim$15 GHz) radio frequencies, existing work has been restricted to the brightest objects, and small sample sizes. For example, past studies demonstrating the link between high-frequency free-free emission and massive star formation include investigations of Galactic star-forming regions (Mezger & Henderson 1967), nearby dwarf irregular galaxies (Klein & Graeve 1986), galaxy nuclei (Turner & Ho 1983, 1994), nearby starbursts (Klein *et al.* 1988; Turner & Ho 1985), and super star clusters within nearby blue compact dwarfs (Turner *et al.* 1998; Kobulnicky & Johnson 1999). And while these studies focus on the free-free emission from galaxies, each was conducted at frequencies $\lesssim$30 GHz. With recent improvements to the backends of existing radio telescopes, such as the Caltech Continuum Backend (CCB) on the Robert C. Byrd Green Bank Telescope (GBT) and the Wideband Interferometric Digital ARchitecture (WIDAR) correlator on the Karl G. Jansky Very Large Array (VLA), the availability of increased bandwidth is making it possible to conduct investigations for large samples of objects at frequencies ∼30 GHz. In this proceeding, we discuss recent results that have taken advantage of these significant electronic upgrades and describe how next-generation radio facilities operating in the ∼1−120 GHz frequency range will provide significantly improved access to the diagnostic information encoded in the radio spectra of galaxies, and in turn transform our understanding of star formation both within and among galaxies.

2. The Energetic Processes Powering Radio Continuum Emission

Radio continuum emission from galaxies covering ∼1−120 GHz is powered by an eclectic mix of physical emission processes, each providing completely independent information on the star formation and ISM properties of galaxies (see Figure 1). These processes include non-thermal synchrotron, free-free (thermal bremsstrahlung), anomalous microwave, and thermal dust emission that are directly related to the various phases of the ISM and provide a comprehensive picture of how galaxies convert their gas into stars. Each of these emission components, described in detail below, are of low surface

https://doi.org/10.1017/S1743921319002898 Published online by Cambridge University Press

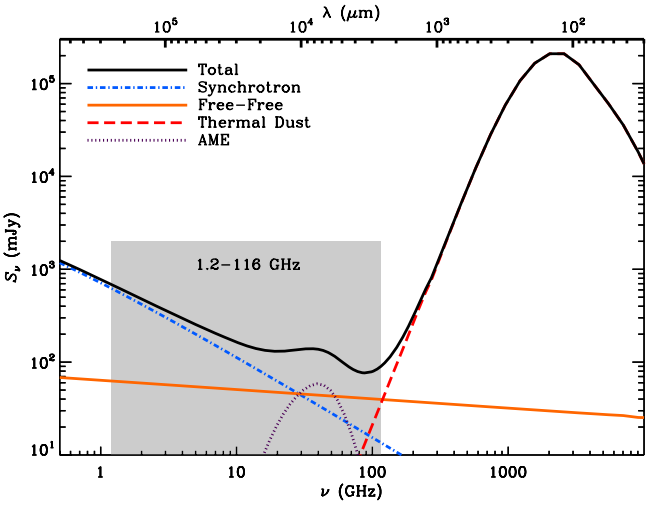

Figure 1. A model spectrum illustrating the various emission processes (non-thermal synchrotron, free-free, AME, thermal dust) that contribute to the observed radio frequency range to be covered by the ngVLA. Only in the proposed ngVLA frequency range (1.2−116 GHz, highlighted) do all major continuum emission mechanisms contribute at similar levels, making this range uniquely well-suited to next-generation continuum studies.

brightness in the ∼30−120 GHz frequency range, and therefore difficult to map in a spatially resolved manner at ∼10−100 pc scales in the general ISM of nearby galaxies using existing facilities. Consequently, our current knowledge about the emissions processes over this frequency range is limited to the brightest star-forming regions/nuclei in the most nearby sources (Leroy *et al.* 2011; Clemens *et al.* 2008, 2010; Murphy 2013; Murphy *et al.* 2015; Barcos-Muñoz *et al.* 2015), providing no information on how the situation may change in drastically different ISM conditions (Tabatabaei *et al.* 2018) that may be more representative of those in high-redshift galaxies, where we have to rely on globally integrated measurements.

The key energetic processes powering radio spectra from star-forming galaxies over the ∼1−120 GHz frequency range include:

• **Non-Thermal Synchrotron Emission:** At ∼GHz frequencies, radio emission from galaxies is dominated by non-thermal synchrotron emission resulting, indirectly, from star formation. Stars more massive than $\sim 8\,M_{\odot}$ end their lives as core-collapse supernovae, whose remnants are thought to be the primary accelerators CR electrons, giving rise to the diffuse synchrotron emission observed from star-forming galaxies. Thus, the synchrotron emission observed from galaxies provides a direct probe of the still barely understood relativistic (magnetic field + CRs) component of the ISM. As illustrated in Figure 1, the synchrotron component has a steep spectral index, typically scaling as $S_{\nu} \propto \nu^{-0.83}$ with a measured rms scatter of 0.13 (Niklas *et al.* 1997). Over the frequency range spanning 1−120 GHz, radio observations will be sensitive to CR electrons spanning more than an order of magnitude in energy (i.e., ∼ 1−50 GeV) for a typical range of ISM magnetic field strengths, including the population that may drive a dynamically-important CR-pressure term in galaxies (Socrates *et al.* 2008).

• **Free-Free Emission:** The same massive stars whose supernovae are directly tied to the production of synchrotron emission in star-forming galaxy disks are also responsible (during their lifetime) for the creation of HII regions. The ionized gas produces free-free emission, which is directly proportional to the production rate of ionizing (Lyman continuum) photons and optically-thin at radio frequencies. In contrast to optical

https://doi.org/10.1017/S1743921319002898 Published online by Cambridge University Press

recombination line emission, no hard-to-estimate attenuation term is required to link the free-free emission to ionizing photon rates, making it an ideal, and perhaps the most reliable, measure of the current star formation in galaxies. Unlike non-thermal synchrotron emission, free-free emission has a relatively flat spectral index, scaling as $S_\nu \propto \nu^{-0.1}$. Globally, free-free emission begins to dominate the total radio emission in normal star-forming galaxies at $\gtrsim$30 GHz (Condon 1992), exactly the frequency range for which the ngVLA will be delivering an order of magnitude improvement compared to any current or planned facility.

• **Thermal Dust Emission:** At frequencies $\gtrsim$100 GHz, (cold) thermal dust emission on the Rayleigh-Jeans portion of the galaxy far-infrared/sub-millimeter spectral energy distribution can begin to take over as the dominant emission component for regions within normal star-forming galaxies. This in turn provides a secure handle on the cold dust content in galaxies, which dominates the total dust mass. For a fixed gas-to-dust ratio, the total dust mass can be used to infer a total gas mass (Heiles *et al.* 1988; Dame *et al.* 2001; Scoville *et al.* 2016). Given the increasingly large instantaneous bandwidth offered by current and planned facilities (e.g., ALMA, ngVLA), such observations will simultaneously provide access to the $J = 1 \rightarrow 0$ line of CO revealing the molecular gas fraction for entire disks of nearby galaxies. Alternatively, combining HI observations with $J = 1 \rightarrow 0$ CO maps, one can instead use the thermal dust emission to measure the spatially varying gas-to-dust ratio directly.

• **Anomalous Microwave Emission (AME):** In addition to the standard Galactic foreground components described above, an unknown component has been found to dominate over these at microwave frequencies between ∼10−90 GHz, and is seemingly correlated with 100 μm thermal dust emission. Cosmic microwave background (CMB) experiments were the first to discover the presence of AME (Kogut *et al.* (1996); Leitch *et al.* 1997), whose origin still remains unknown (for a review, see Dickinson *et al.* 2018). Its presence as a foreground is problematic as the precise characterization and separation of foregrounds remains a major challenge for current and future CMB experiments (BICEP2/Keck Collaboration *et al.* 2015; Planck Collaboration *et al.* 2016). At present, the most widely accepted explanation for AME is the spinning dust model (Erickson 1957; Draine & Lazarian 1998; Planck Collaboration *et al.* 2011; Hensley & Draine 2017) in which rapidly rotating very small grains, having a nonzero electric dipole moment, produce the observed microwave emission. Increasing the mapping speed at these frequencies with future instruments will lead to unprecedented investigations into the origin and prominence of this emission component both within our own galaxy and others, ultimately helping to improve upon the precision of future CMB experiments.

3. Recent Results

Murphy *et al.* (2012) presented 33 GHz photometry of 103 galaxy nuclei and extranuclear star-forming regions taken with the CCB on the GBT as part of the Star Formation in Radio Survey (SFRS). This study was limited to the 25″ resolution of the GBT beam at 33 GHz, which corresponds to a linear scale of ∼1 kpc given the typical distance of the SFRS galaxies. Among the sources without evidence for an active galactic nucleus, and also having lower frequency radio data available, the median thermal fraction at 33 GHz was ≈76% with a dispersion of ≈24%. For all sources resolved on scales $\lesssim$0.5 kpc, the thermal fraction was found to be even larger at $\gtrsim$90% suggesting that radio emission at 33 GHz provides a sensitive measure of the ionizing photon rate from young star-forming regions. The 33 GHz to total IR flux ratio was found to increase as the radio spectral index (measured between 1.7 and 33 GHz) flattens independent of the GBT projected beam area. Consequently, the ratio of non-thermal to total IR emission

https://doi.org/10.1017/S1743921319002898 Published online by Cambridge University Press

appears relatively constant on $\gtrsim$1 kpc scales, suggesting only moderate variations in the cosmic-ray electron injection spectrum and ratio of synchrotron to total cooling processes among star-forming complexes. Assuming that this trend solely arises from an increase in the thermal fraction sets a maximum on the scatter of the non-thermal spectral indices among the star-forming regions of $\sigma_{\alpha^{\rm NT}} \lesssim 0.13$, consistent with Niklas *et al.* (1997).

This work was been recently advanced though new 33 GHz imaging for the SFRS using the VLA, mapping 112 pointings on $\gtrsim 2''$ scales, compared to the $\approx 25''$ single-beam GBT photometry. These galaxies, which are included in the *Spitzer* Infrared Nearby Galaxies Survey (SINGS; Kennicutt *et al.* 2003) and Key Insights on Nearby Galaxies: a Far-Infrared Survey with *Herschel* (KINGFISH; Kennicutt *et al.* 2011) legacy programs, are well studied and have a wealth of ancillary data available. A comparison with 33 GHz GBT single-dish observations indicates that the interferometric VLA observations recover $78\% \pm 4\%$ of the total flux density over $25''$ regions ($\approx$kpc scales) among all fields. On these scales, the emission being resolved out is most likely diffuse non-thermal synchrotron emission. Consequently, on the $\approx$30–300 pc scales sampled by VLA observations, the bulk of the 33 GHz emission is recovered and primarily powered by free-free emission from discrete HII regions, making it an excellent tracer of massive star formation. Of the 225 discrete regions used for aperture photometry, 162 are extranuclear (i.e., having galactocentric radii $r_{\rm G} \gtrsim 250$ pc) and detected at $> 3\sigma$ significance at 33 GHz and in Hα. Assuming a typical 33 GHz thermal fraction of 90% based on previous GBT results, the ratio of optically-thin 33 GHz to uncorrected Hα SFRs indicates a median extinction value on $\approx$30–300 pc scales of $A_{\rm H\alpha} \approx 1.26 \pm 0.09$ mag, with an associated median absolute deviation of 0.87 mag. Roughly 10% of these sources are highly embedded (i.e., $A_{\rm H\alpha} \approx\gtrsim$ 3.3 mag), suggesting that on average, HII regions remain embedded for $\lesssim$1 Myr.

New complementary interferometric observations at approximately matched resolution in the S- (2−4 GHz) and Ku- (12−18 GHz) bands (VLA/13B-215; PI. Murphy) has extended this analysis by allowing for the construction of spectral index maps for all regions which in turn results in a much more robust thermal/non-thermal decompositions (Linden *et al.* 2020). In the left panel of Figure 2, spectral index distributions are shown for frequencies between 3 and 15 GHz, 15 and 33 GHz, as well as measured via a ordinary least squares fit across all three frequencies for those sources detected in at least two of the three radio maps. Median and standard deviation (rms) values are given for each distribution, which are fairly consistent suggesting that the spectrum does not exhibit much curvature. Some spectral indices appear to be flatter than what is expected from pure free-free emission, and even positive in some cases. Such instances may be the result of a chance GHz peaking background galaxy, or perhaps due to AME (e.g., Murphy *et al.* 2010, 2018b), and will be followed up.

For 329 sources detected in at least two of the three radio maps, the typical aperture diameter used for the photometry corresponds to a median linear scale of $\approx$150 pc. Using the spectral index information over this lever-arm (that is an order-of-magnitude in frequency), we can estimate the thermal emission fraction at 33 GHz if we assume a fixed non-thermal spectral index. A constant non-thermal radio spectral index of $\alpha^{\rm NT} = 0.83$ is assumed given that this is the value found by Niklas *et al.* (1997; i.e., $\alpha^{\rm NT} = 0.83$ with a scatter of $\sigma_{\alpha^{\rm NT}} = 0.13$) and consistent to the average non-thermal spectral index found among the 10 star-forming regions studied in NGC 6946 by Murphy *et al.* (2011). For sources with measured spectral indices steeper than −0.83, that value less by −0.1 is used. In the right panel of Figure 2 the resulting distribution of the 33 GHz thermal fractions is shown, having median thermal fraction at 33 GHz is $\approx$93% with an rms of $\approx$24%. It is possible that circum-nuclear sources in the sample may be contaminated by energetics not associated with star formation. Limiting the analysis to only the 291

https://doi.org/10.1017/S1743921319002898 Published online by Cambridge University Press

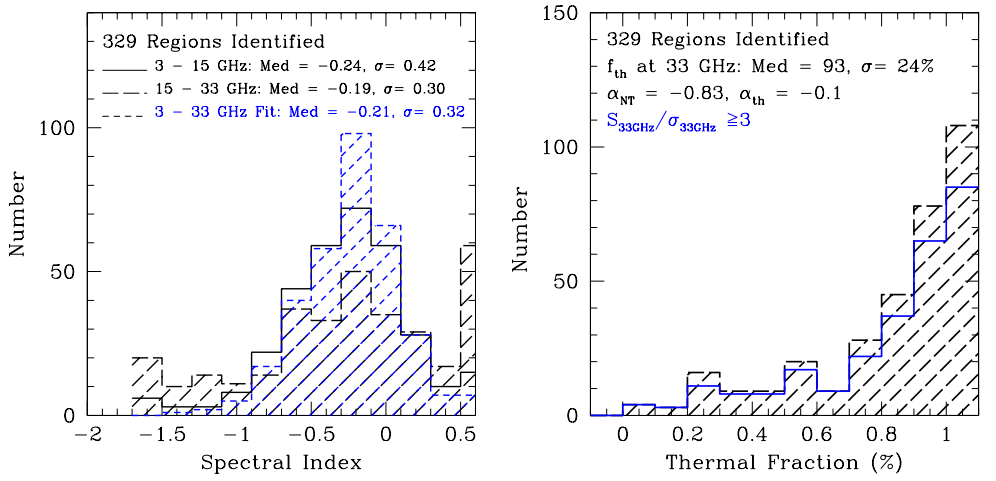

Figure 2. Adapted from Linden *et al.* (2020), which we refer the reader to for final plots and results. *Left:* The spectral index distributions measured between 3 and 15 GHz, 15 and 33 GHz, and measured via a ordinary least squares fit across all three frequencies measured at a common (i.e., the lowest) resolution of the native of the radio maps. Median and standard deviations (rms) values are given for each distribution. For the 329 sources detected in at least two of the three radio maps, this corresponds to a median linear scale of ≈150 pc *Right:* The corresponding distribution of thermal fractions measured at 33 GHz for all 329 sources assuming a non-thermal spectral index of −0.83 (Niklas *et al.* 1997; Murphy *et al.* 2011). With a median value of ≈93% and a standard deviation (rms) of ≈24%, the 33 GHz flux density appears to be a very sensitive measure of the ionizing flux of these star-forming regions.

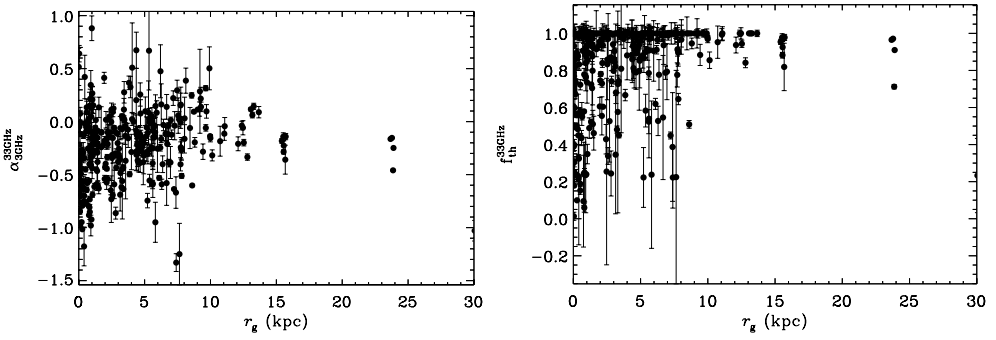

Figure 3. Adapted from Linden *et al.* (2020), which we refer the reader to for final plots and results. *Left:* Spectral index plotted against galactodentric radius. *Right:* Thermal fraction at 33 GHz plotted agains galactocentric radius. The scatter in spectral index (and thermal fraction) appears to decrease with increasing galactocentric radius.

sources with $r_G \gtrsim 250$ pc results in a similar value for the median 33 GHz thermal fraction, being ≈96% with an rms of ≈23%. Consequently, on the scales of $\lesssim$ a few hundred pc, the 33 GHz flux density appears to be dominated by free-free emission and therefore a sensitive measure of the ionizing flux of newly formed massive stars.

What is also found is that the scatter in spectral indices and thermal fractions decreases with increasing r_G (Figure 3). This result most likely arises from different star formation histories in the centers of galaxies versus further out in the disk, with the galaxy centers have longer periods of ongoing star formation. This in turn results in a larger spread of ages and radio spectral indices, as well as populations of CR electrons/positrons to be (re-)accelerated by passing shocks from next-generation star formation events.

https://doi.org/10.1017/S1743921319002898 Published online by Cambridge University Press

4. Prospects with Future Facilities – A next-generation VLA

In the 2020's there will be a powerful suite of next-generation radio/mm facilities available that will transform our understanding in many areas of astrophysics. As currently envisioned, phase one of the Square Kilometre Array (SKA1-MID) will be the premier radio interferometer at decimetric wavelengths, consisting of up to 133 15 m (+ 64 13.5 m MeerKAT) dishes with a maximum baseline of up to ∼150 km and eventually covering a frequency range spanning 350 MHz (85 cm) to 14 GHz (2 cm). ALMA, on the other hand, is a radio interferometer optimized to take advantage of the sub-mm (THz) windows that are only accessible at high, dry sites such as the Chajnantor plateau, which is at ∼5000 m altitude. The currently envisioned next-generation Very Large Array (ngVLA) will be optimized for observations at frequencies (i.e., 1.2−116 GHz) between the exquisite performance of ALMA at submm wavelengths, and the future SKA-1 at decimeter to meter wavelengths, thus lending itself to be highly complementary with these facilities.

The ngVLA will revolutionize our understanding of the emission mechanisms that power the radio continuum emission in and around galaxies by enabling the routine construction of ∼1.2−116 GHz radio spectral maps. Coupled with its nearly order of magnitude increased sensitivity compared to the current VLA, the ngVLA will make it possible to use this frequency window to investigate the distinct physical processes linked to stellar birth and death for large, heterogeneous samples of galaxies. Delivering such a finely sampled spectrum over this entire frequency range with a single instrument will allow robust separation of the various emission components, which is currently the main challenge for multi-frequency radio studies. Each observation will provide enough sensitivity and spectral coverage to robustly decompose and accurately quantify the individual energetic components powering the radio continuum, thus providing unique information on the non-thermal plasma, ionized gas, and cold dust content in the disks and halos of galaxies.

4.1. *Mapping Star Formation within Nearby Galaxies on a Range of Physical Scales*

For a proper decomposition of the radio continuum emission into its component parts, one needs to have spectral coverage at frequencies low enough (i.e., < 10 GHz) to be dominated by the non-thermal, steep (i.e., $\alpha \approx -0.8$) spectrum component, and at frequencies high enough (i.e., > 50 GHz) where the emission becomes completely dominated by the flat (i.e., $\alpha \approx -0.1$) spectrum free-free emission. Given the potential for a significant contribution from AME (Murphy *et al.* 2010, 2018b; Scaife *et al.* 2010; Hensley *et al.* 2015), peaking at frequencies $\sim 20-40$ GHz, coarse coverage spanning that spectral region is critical to account for such features. To date, the shape of the AME feature is largely unconstrained, and has not been carefully measured in the ISM of extragalactic sources. This is largely due to the insensitivity of current facilities to conduct a proper search for AME in nearby galaxies and map the feature with enough frequency resolution to provide useful constraints on its shape.

Broadband imaging spanning a frequency range of $1 - 120$ GHz (i.e., largely covered by the ngVLA) will therefore be extremely powerful to properly decompose radio continuum emission from galaxies into its constituent parts. Additionally having frequency coverage below ∼10 GHz provides sensitivity to free-free absorption, which is common in nearby luminous infrared galaxies (Condon *et al.* 1991; Clemens *et al.* 2010; Barcos-Muñoz *et al.* 2015). For individual (ultra compact) HII regions, the turnover frequency can be as high as ≈20 GHz (Murphy *et al.* 2010). A fundamental goal of the ngVLA will be to produce star formation maps for a large, heterogenous samples of nearby galaxies at $\approx 1''$ resolution. This will deliver Hα-like images that optical astronomers have relied on heavily for decades without having the additional complications of extinction and contamination by nearby [NII] emission, which make such images challenging to interpret.

https://doi.org/10.1017/S1743921319002898 Published online by Cambridge University Press

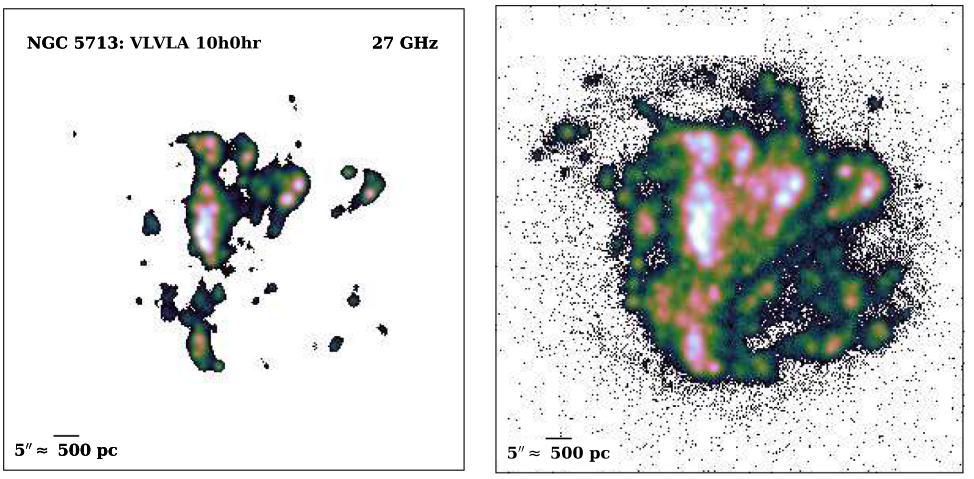

Figure 4. Both panels show a model 27 GHz free-free emission image of NGC 5713 ($d_L \approx 21.4$ Mpc, SFR $\approx 4\,M_\odot\,\mathrm{yr}^{-1}$) based on an existing H$\alpha$ narrow band image at its native ($\approx 1''$) angular resolution taken from SINGS (Kennicutt *et al.* 2003). The left and right panels indicate the emission that would be detected at the 3σ level after a 10 hr on-source integration time using the current VLA in C-configuration ($1\sigma \approx 1.5\,\mu\mathrm{Jy\,bm}^{-1}$) and the ngVLA with a $1''$ sculpted beam ($1\sigma \approx 0.17\,\mu\mathrm{Jy\,bm}^{-1}$). In a relatively modest integration, the ngVLA is able to recover a significant fraction of star formation activity that is completely missed by the VLA.

By achieving arcsecond-like resolution that is commensurate with ground-based optical facilities, the ngVLA will be able to probe ≈100 pc scales out to the distance of Virgo (the nearest massive cluster at $d \approx 16.6$ Mpc), which are the typical sizes of giant molecular clouds (GMCs) and giant HII regions. At an rms sensitivity of $0.15\,\mu\mathrm{Jy\,bm}^{-1}$ at 27 GHz, such radio maps will reach a sensitivity expressed in terms of SFR density of $\approx 0.005\,M_\odot\,\mathrm{yr}^{-1}\mathrm{kpc}^{-2}$, matching the sensitivity of extremely deep Hα images such as those included in the Local Volume Legacy survey (Kennicutt *et al.* 2008). An example of this is illustrated in Figure 4 where an existing Hα narrow band image taken from SINGS (Kennicutt *et al.* 2003) was used to create a model 27 GHz free-free emission map at $1''$ resolution for the nearby star-forming galaxy NGC 5713. With a 10 hr integration the ngVLA will be able to map the entire disk of NGC 5713 down to an rms of $\approx 0.15\,\mu\mathrm{Jy\,bm}^{-1}$ (≈35 mK). A comparison of what can currently be delivered with the VLA for the same integration time is also shown, indicating that only the brightest star-forming peaks are able to be detected. To make a map to the same depth using the current VLA would take ≳800 hr! This is the same amount of time it would take to roughly survey ≳80 galaxies with the ngVLA.

Using the same data, but applying a different imaging weighting scheme to create finer resolution maps (i.e., $0\farcs1$, or even higher for brighter systems), similar multi-frequency radio continuum analyses can be performed for discrete HII regions and supernova remnants (SNRs) to complement high-resolution, space-based optical/NIR observations (e.g., *HST*, *JWST*, *WFIRST*, etc.). At an angular resolution of $0\farcs1$, the data would sample ≈10 pc scales in galaxies out to the distance of Virgo to resolve and characterize (e.g., size, spectral shape, density, etc.) discrete HII regions and SNRs with a sensitivity to diffuse free-free emission corresponding to a SFR density of $\approx 0.5\,M_\odot\,\mathrm{yr}^{-1}\mathrm{kpc}^{-2}$.

Consequently, the ngVLA will provide a transformational step for studies of star formation in the local universe covering a large, heterogeneous set of astrophysical conditions. This statement is independent of the fact that with such observations using the ngVLA, having its wide-bandwidth, a number of RRL's will come for free. The detection of such lines (individually or through stacking), coupled with the observed continuum emission,

https://doi.org/10.1017/S1743921319002898 Published online by Cambridge University Press

can be used to quantify physical conditions for the HII regions such as electron temperature. It is without question that the ngVLA will make radio observations a critical component for investigations carried out by the entire astronomical community studying star formation and the ISM of nearby galaxies.

5. Summary

Radio spectra are powered by a combination of energetic processes, each of which contains a wealth of diagnostic information. By taking advantage of new wide-frequency backend capabilities of current radio facilities, observations of faint, high-frequency (i.e., $\gtrsim 30$ GHz) radio emission has become possible for samples of relatively bright regions within nearby galaxies. Such studies have shown that emission at these frequencies is dominated by free-free emission, being $\gtrsim$90% on $\lesssim$ a few hundred pc scales, making it a highly sensitive measurement of the ionizing photon rate of massive stars. To substantially advance these studies will take next-generation facilities covering frequencies spanning $\sim$1$-$120 GHz, such as the ngVLA. With an order-of-magnitude improvement in sensitivity over current and planned facilities at these frequencies, the ngVLA will enable transformational advancements in studies of star formation in the local universe and complement studies carried out with contemporaneous facilities like the SKA1 and ALMA, creating the ultimate suite of radio telescopes.

Acknowledgement

EJM thanks S. Linden for helping prepare figures from our currently unpublished work.

References

Barcos-Muñoz, L., Leroy, A. K., Evans, A. S., *et al.* 2015, *ApJ*, 799, 10
Barger, A., Kohno, K., Murphy, E. J., *et al.* 2018, ASP Monograph 7, Title of the Book, ed. E. Murphy (San Francisco, CA: ASP)
Balser, D. S., Anderson, L. D., Bania, T. M., *et al.* 2018, ASP Monograph 7, Title of the Book, ed. E. Murphy (San Francisco, CA: ASP)
BICEP2/Keck Collaboration, Planck Collaboration, Ade, P. A. R., *et al.* 2015, Physical Review Letters, 114, 101301
Bot, C., Ysard, N., Paradis, D., *et al.* 2010, *A&A*, 523, A20
Clemens, M. S., Vega, O., Bressan, A., *et al.* 2008, *A&A*, 477, 95
Clemens, M. S., Scaife, A., Vega, O., & Bressan, A. 2010, *MNRAS*, 405, 887
Condon, J. J. & Yin, Q. F. 1990, *ApJ*, 357, 97
Condon, J. J., Huang, Z.-P., Yin, Q. F., & Thuan, T. X. 1991, *ApJ*, 378, 65
Condon, J. J. 1992, *ARA&A*, 30, 575
Dame, T. M., Hartmann, D., & Thaddeus, P. 2001, *ApJ*, 547, 792
Dickinson, C., Ali-Haïmoud, Y., Barr, A., *et al.* 2018, NewAR, 80, 1
Draine, B. T. & Lazarian, A. 1998, *ApJL*, 494, L19
—. 1999, *ApJ*, 512, 740
Erickson, W. C. 1957, *ApJ*, 126, 480
Heiles, C., Reach, W. T., & Koo, B.-C. 1988, *ApJ*, 332, 313
Hensley, B., Murphy, E., & Staguhn, J. 2015, *MNRAS*, 449, 809
Hensley, B. S., Draine, B. T., & Meisner, A. M. 2016, *ApJ*, 827, 45
Hensley, B. S. & Draine, B. T. 2017, *ApJ*, 836, 179
Klein, U. & Graeve, R. 1986, *A&A*, 161, 155
Klein, U., Wielebinski, R., & Morsi, H. W. 1988, *A&A*, 190, 41
Kennicutt, Jr., R. C., Armus, L., Bendo, G., *et al.* 2003, *PASP*, 115, 928
Kennicutt, R. C., Jr., Lee, J. C., Funes, J. G., *et al.* 2008, *ApJS*, 178, 247–279
Kennicutt, R. C., Calzetti, D., Aniano, G., *et al.* 2011, *PASP*, 123, 1347
Kobulnicky, H. A. & Johnson, K. E. 1999, *ApJ*, 527, 154
Kogut, A., Banday, A. J., Bennett, C. L., *et al.* 1996, *ApJ*, 460, 1

Koyama, K., Petre, R., Gotthelf, E. V., *et al.* 1995, *Nature*, 378, 255
Leroy, A. K., Evans, A. S., Momjian, E., *et al.* 2011, *ApJL*, 739, L25
Leitch, E. M., Readhead, A. C. S., Pearson, T. J., & Myers, S. T. 1997, *ApJL*, 486, L23
Linden, S. T., Murphy, E. J., Dong, D., *et al.* 2020, *ApJS*, submitted
Mezger, P. G. & Henderson, A. P. 1967, *ApJ*, 147, 471
Murphy, E. J., Helou, G., Condon, J. J., *et al.* 2010a, *ApJL*, 709, L108
Murphy, E. J., Condon, J. J., Schinnerer, E., *et al.* 2011, *ApJ*, 737, 67
Murphy, E. J., Bremseth, J., Mason, B. S., *et al.* 2012, *ApJ*, 761, 97
Murphy, E. J. 2013, *ApJ*, 777, 58
Murphy, E. J., Dong, D., Leroy, A. K., *et al.* 2015, *ApJ*, 813, 118
Murphy, E. J., Momjian, E., Condon, J. J., *et al.* 2017, *ApJ*, 839, 35
Murphy, E. J., Dong, D., Momjian, E., *et al.* 2018a, *ApJS*, 234, 24
Murphy, E. J., Linden, S. T., Dong, D., *et al.* 2018b, *ApJ*, 862, 20
Murphy, T., Cohen, M., Ekers, R. D., *et al.* 2010b, *MNRAS*, 405, 1560
Niklas, S., Klein, U., & Wielebinski, R. 1997, *A&A*, 322, 19
Peel, M. W., Dickinson, C., Davies, R. D., Clements, D. L., & Beswick, R. J. 2011, *MNRAS*, 416, L99
Planck Collaboration, Ade, P. A. R., Aghanim, N., *et al.* 2011, *A&A*, 536, A20
Planck Collaboration, Adam, R., Ade, P. A. R., *et al.* 2016, *A&A*, 586, A133
Scaife, A. M. M., Nikolic, B., Green, D. A., *et al.* 2010, *MNRAS*, 406, L45
Scoville, N., Sheth, K., Aussel, H., *et al.* 2016, *ApJ*, 820, 83
Selina, R. and Murphy, E. J., 2017, ngVLA Memo #17
Socrates, A., Davis, S. W., & Ramirez-Ruiz, E. 2008, *ApJ*, 687, 202–215
Tabatabaei, F. S., Minguez, P., Prieto, M. A., & Fernández-Ontiveros, J. A. 2018, *Nature Astronomy*, 2, 83
Turner, J. L. & Ho, P. T. P. 1983, *ApJL*, 268, L79
—. 1985, *ApJL*, 299, L77
—. 1994, *ApJ*, 421, 122
Turner, J. L., Ho, P. T. P., & Beck, S. C. 1998, *AJ*, 116, 1212

Discussion

Rosario: Given the range in radio spectral shapes and thermal fractions in individual SF regions, can you reflect on how much uncertainty one must keep in mind when using radio measurements as SF tracers in higher redshift surveys?

Murphy: This question really requires 2 answers. In the case where the IMF is known and the galaxy being studied is known to be star-forming (not an AGN), the uncertainty on the radio derived SFR is quite good, and will be more reliable for higher frequency observations (say $\sigma_{\rm SFR} < 2\times$, and perhaps as good as 20-50% uncertainty). If one folds in the uncertainty in the IMF and/or the contribution from an AGN, the uncertainty is $> 2\times$, just like any other SFR diagnostic.

Schaerer: When going to higher redshifts, we are interested in compact SFGs, maybe resembling low-z dwarfs. How do these fit into the observation and trends you have shown?

Murphy: Such galaxies should be detectable in the radio. Depending on how porous these galaxies are to cosmic rays, they may only be detectable in their free-free emission.

Nagao: Are radio spectra of ULIRGs free from possible AGN contributions? Removing very low-luminosity AGNs from the ULRIG sample may be difficult.

Murphy: It is almost certain that ULRIGs will contain some fraction of radio emission that is due to AGN. However, determining the fraction (or dominance) can be carried out using other diagnostics. In the case of what was presented, PAH equivalent widths were used, which I believe has reliably determined those sources denoted by AGN.